Hindawi Publishing Corporation
International Journal of Photoenergy
Volume 2007, Article ID 32859, 8 pages
doi:10.1155/2007/32859

Research Article

Photocatalytic Degradation of Toluene in Air Using a Fluidized Bed Photoreactor

O. Prieto,[1] J. Fermoso,[1] and R. Irusta[1,2]

[1] *CARTIF Foundation, Technology Park, 47151 Valladolid, Boecillo, Spain*
[2] *Department of Chemical Engineering and Environmental Technology, School of Industrial Engineering, University of Valladolid, 47011 Valladolid, Spain*

Received 16 February 2006; Revised 9 January 2007; Accepted 9 January 2007

Recommended by Sabry Abdel-Mottaleb

The photocatalytic degradation of toluene in air was carried out on particles of TiO_2 in a photocatalytic reactor that had been developed to study the treatment of organic pollutants in a gaseous phase. Hypothetically, the fluidized bed technology of this reactor could make it possible to increase the mass transfer coefficients in comparison with those of conventional photoreactors. The photocatalytic particles used were prepared by mixing TiO_2 (Degussa P25) and starch in a methanol solution. The XRD and SEM results of these aggregates confirm the titanium dioxide (Degussa P25) characteristics, such as the presence of anatase on the particle surface and spongy and wrinkled morphology. Toluene concentrations varied from 0.9 to 199 ppm_v, and all the experiments were carried out with a flow rate of 300 NL/h. Toluene conversions from 77% to 100% were obtained in the range studied. In this work, the regeneration processes of deactivated TiO_2 photocatalysts have been investigated using FT-IR and GC/MS techniques. Benzoic acid, benzaldehyde, and benzyl alcohol were the three major intermediate products identified.

1. INTRODUCTION

Volatile organic compounds (VOCs) are an important category of air pollutants present in the atmosphere of all urban and industrial areas. Toluene is one of the major indoor and industrial air pollutants and several strategies have been identified in order to reduce its presence in civil and industrial emissions. Among the methods to oxidize toluene, heterogeneous photocatalysis is one of the most attractive, due to the mild operational conditions usually employed in the experiments.

Photocatalysis is an advanced oxidation process in which the energy required is supplied by the direct absorption of UV radiation at room temperature, and needs the use of semiconductor materials with an adequate band gap as a photocatalyst. Titanium dioxide (TiO_2) is the most attractive semiconductor, because of its high photocatalytic efficiency, its stability against photo-corrosion and chemicals, its low toxicity, and its low cost. Its band-gap energy of 3.2 eV leads to its photoexcitation which requires wavelengths of less than ca. 385 nm, corresponding to a near-UV irradiation. The absorption of UV radiation excites electrons from the valence to the conduction band, creating electron-hole pairs with a high oxidative potential of 3 eV associated with the holes photogenerated, which initiate redox reactions with adsorbed surface species [1]. The idea of using a fluidized bed as both a uniform radiation distribution and an immobilized support for photocatalysts was originally proposed and theoretically evaluated by Yue et al. [2]. Some authors [3–5] have demonstrated the experimental application of this idea. Fluidized bed photocatalytic reactor systems have several advantages compared to conventional immobilized photocatalytic reactors. Reactor configuration provides both exposure of the photocatalyst to UV radiation and good penetration of the radiation in the photocatalyst bed that improves the contact of the photocatalyst with the gas [6]. When a particle bed is expanded from a fixed bed, particles are more separated and the screening effect of the radiation is less important. A higher gas velocity implies a higher bed expansion and void fraction.

In the present study, a particular TiO_2 photocatalyst (Degussa P25) has been synthesized and characterized in order to be used in the degradation of toluene in a fluidized bed photoreactor. At the same time, attention was focused on identification of intermediate products present on the surface of the exhausted TiO_2 photocatalyst and on its regeneration.

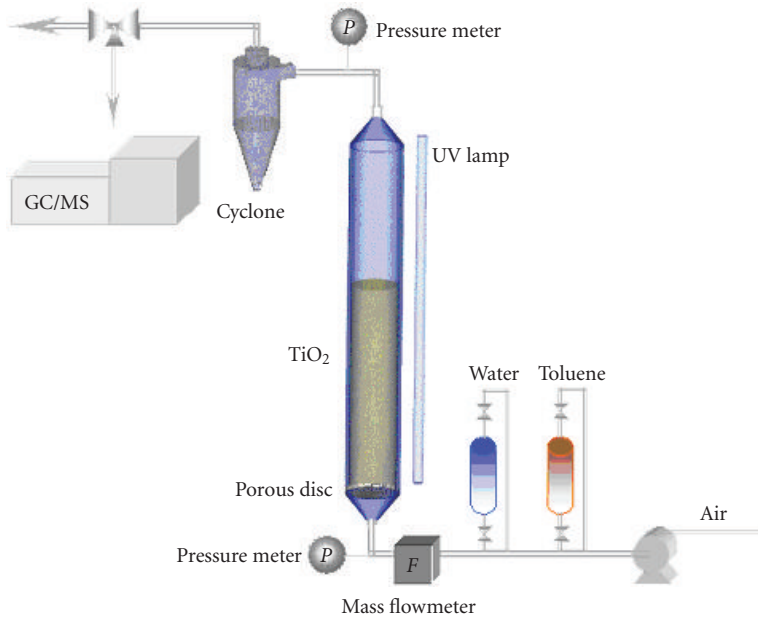

Figure 1: Schematic diagram of the fluidized bed photoreactor.

2. EXPERIMENTAL

2.1. Reagents and catalyst preparation

Toluene (PA), methanol (ACS), and starch (soluble, synthesis grade) were purchased from Panreac Química S.A., Spain, and used without further purification.

The catalyst powder was TiO_2 Degussa P25, which was employed as received without further treatment. TiO_2 Degussa P25 particles were approximately spherical and nonporous with a purity over 99.5% and are reported to contain about 80% of anatase and 20% of rutile. Therefore, starch was used as a binder, in order to obtain more abrasion-resistant particles. The use of starch has been proposed in order to overcome the problems associated with the poor fluid dynamic properties of the titanium catalyst. P25 powder is classified within the Geldart C group (according to its particle size and density) having a poor fluidization behavior.

The catalysts used in the fluidized bed photoreactor were developed by mixing TiO_2 (Degussa P25) with starch in 800 ml of distilled water and a methanol solution (50% v/v) and then stirring until a homogeneous phase was obtained. The TiO_2/starch relation (w/w) used was 15. The resulting solution was vigorously stirred using a magnetic stirrer until a homogeneous solution was formed. Then, the mixture was dried overnight in an open oven at 110°C and calcined in air at 400°C for 2 hours. Finally, the sample was crushed and sieved to a suitable particle size to be fluidized (between 0.5 and 0.25 mm). The particles obtained were nonporous and nonspherical with an apparent density of 1.39 g cm^{-3}.

2.2. Fluidized bed photoreactor

The photocatalytic reactions were carried out in a fluidized bed photoreactor. As shown in Figure 1, this cylindrical reactor is a quartz glass tube of 40 mm ID (inner diameter) and 665 mm high. A Pyrex porous disc was used as a distributor to provide the uniform fluidization of the TiO_2 photocatalyst. A low-pressure mercury vapor ultraviolet lamp (40 W, Philips TLK40W/10-R) was installed outside as the source of UV radiation. The wavelength of the UV lamp ranges from 300 to 400 nm with the peak of maximum radiation intensity at 365 nm.

In order to obtain the toluene concentration, an air stream was passed through a saturator with toluene and then diluted by the main air stream to adjust the toluene concentration. A similar device was used to evaporate the water but with a higher flow.

The flow rate of the carrying gas (air) was measured using a mass flow-meter (D-6200 M + W Instruments). Concentration of the toluene was measured using an online gas chromatograph (Agilent 6890N) equipped with a mass detector (Agilent 7953N) and an autosampling valve system. No photocatalytic degradation products, CO, CO_2, could be determined with this equipment.

The minimum fluidization velocity (U_{mf}) of the TiO_2 photocatalyst particles was determined by graphically plotting their pressure drop versus the inlet gas velocity (U_g). The minimum fluidization velocity is the minimum velocity of the superficial gas which makes the particle bed act as a fluid-like state through contact with a gas stream. Below the minimum fluidization velocity the gas will flow through channels between the particles.

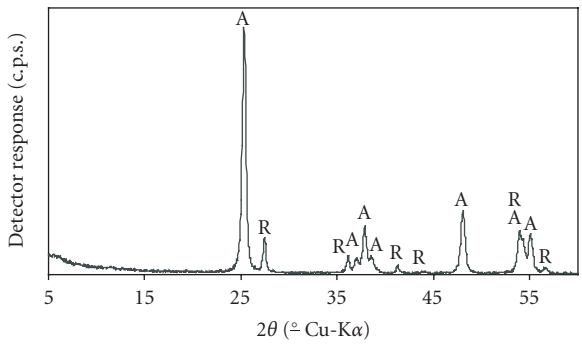

FIGURE 2: XRD patterns of aggregates of TiO_2 particles (A: anatase and R: rutile).

2.3. Catalyst characterization

Samples have been studied using the following characterization techniques: crystalline structure phases were determined using X-ray diffraction (XRD) in a Philips PW1710 powder diffractometer in the 5–75° (2θ) region using Cu-Kα radiation ($\lambda = 1.54050$ Å). FT-IR spectra were recorded in a Bruker Tensor 27 with Golden Gate (SPECAC). Textural and morphological properties were analyzed by nitrogen adsorption in an Omnisorp 100CX Coulter. Electronic images were obtained in a JEOL JSM-820 microscope. Samples were prepared and placed on a conductive double faced adhesive and then covered by another layer in an evaporating Balzers SDC040. The elemental analysis of carbon, hydrogen, and nitrogen was performed on a Leco instrument, model CHN-600.

3. RESULTS AND DISCUSSION

3.1. Characterization of the TiO_2 photocatalyst

The powder X-ray diffraction patterns of aggregates of TiO_2 particles are shown in Figure 2. As can be seen in the XRD pattern, the photocatalyst has strong anatase diffraction peaks at $2\theta \approx 25.3°$; 37.8°; and 48.0° corresponding to diffraction planes (101), (004), and (200), respectively, as well as small rutile diffraction peaks at $2\theta \approx 27.4°$; 36.0°; and 41.2°, corresponding to the diffraction planes (110), (101), and (111), respectively.

The nature and distribution of the TiO_2 superficial OH group is often the determining factor of the catalytic behavior. The spectrum of aggregates of TiO_2 particles (Figure 3) is characterized by a series of narrow components in the 3800–3600 cm^{-1} range. In our case, peaks are observed at 3692 cm^{-1} due to vibrations of isolated OH groups and an intense and broad absorption in the 3600–3200 cm^{-1} range, with a maximum at 3278 cm^{-1}, resulting from the superposition of the $_\nu$OH mode of bonded hydroxyl groups and of the symmetric and antisymmetric $_\nu$OH modes of molecular water coordinated to Ti^{4+} ions as cations on (110) face of microcrystalline rutile [7]. The band at 1626 cm^{-1} is assigned to the OH bend vibrations ($_\delta$OH). The absorption bands at ca. 2922 and 2838 cm^{-1} refer to the C−H stretching due to

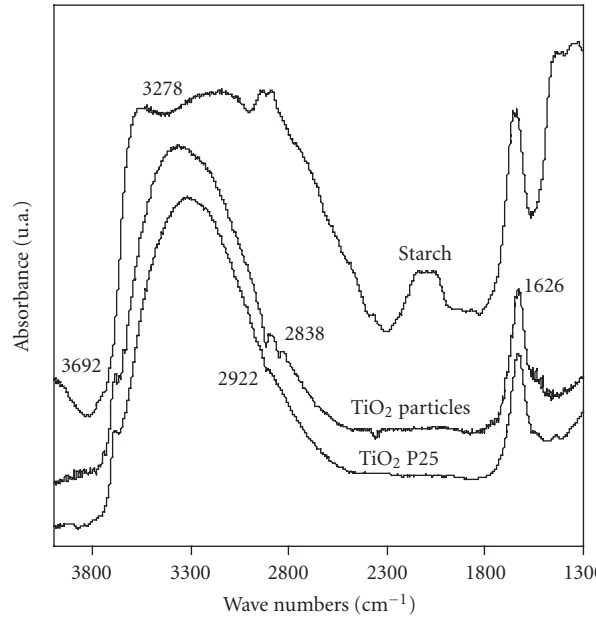

FIGURE 3: FT-IR spectra of TiO_2 particles aggregates, TiO_2 P25, and starch. The spectra have been displaced vertically for clarity.

the remaining organic compounds. Thus, it could indicate that organic residues of the starch remain at 400°C. However, according to the elemental analysis of C, H, and N of the sample, the amount of C is lower than 0.1% w. We therefore consider that this minimum amount of starch does not affect the photocatalyst activity.

The SEM pictures of the aggregates of TiO_2 particles contain the spongy and wrinkled morphology characteristic of the TiO_2 P25 (Figure 4(a)). However, there are also particles greater than TiO_2 (Degussa P25) in size. These agglomerates enhance the fluidization behavior but are responsible for a reduction of the BET surface sample from 50 m^2/g of P25 to 46 m^2/g of the aggregates of TiO_2 particles.

3.2. Activity test

Toluene degradation via photocatalysis was carried out in a fluidized bed photoreactor with different initial toluene concentrations in air. The initial toluene concentrations used in the experimentation varied from 0.9 to 199 ppm_ν. All the experiments were carried out with a flow rate of 300 NL/h which would suggest a residence time of 4.52 seconds. The same amount of fresh catalyst, 225 g, was used in each experiment. Once system stabilization was achieved, each experiment was carried out between six and eight hours without reduction in the catalyst efficiency. Toluene removal yield is calculated as the mean of the set of values recorded during this time.

As can be seen in Figure 5, relative toluene photodegradation decreased when the initial toluene concentration was increased. 100% toluene was degraded when its concentration in the reactor ranged from 0.9 to 4 ppm_ν. Nevertheless, the removal obtained with 200 ppm_ν was only 77%.

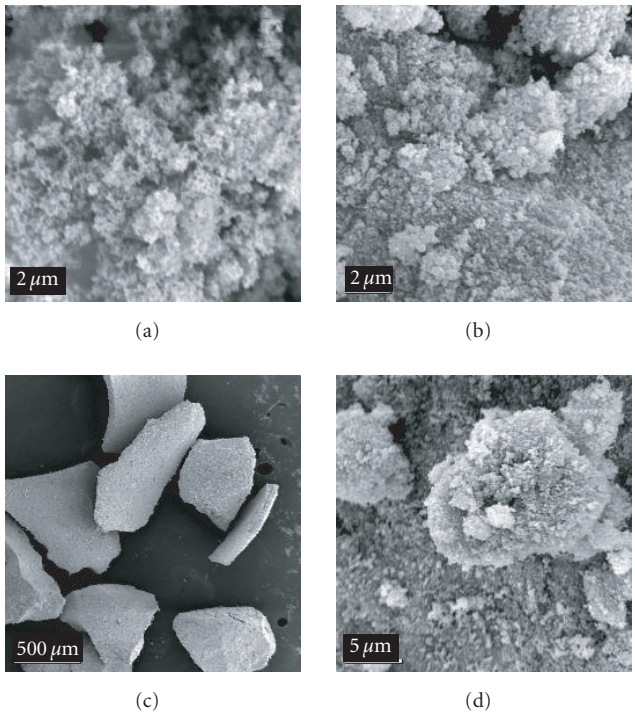

Figure 4: SEM pictures of TiO_2 P25 samples (a) and aggregates of TiO_2 particles (b), (c), and (d).

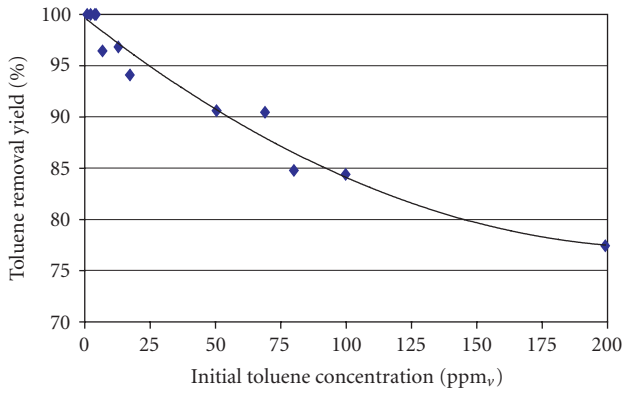

Figure 5: Variation of the toluene removal yield versus the initial toluene concentration.

In Table 1 we show a comparative study between the above-mentioned data and the results obtained by other authors who have assessed the gas phase photocatalytic removal of toluene.

Marcì et al. [8] carried out a degradation of toluene in a Carberry-type photoreactor with a flow rate of 120 L/h (two orders of magnitude higher than the one usually employed in a fixed bed photoreactor). Under these conditions a 5% toluene conversion ($9.78 \cdot 10^{-3}$ mg/m$^2 \cdot$ s) was obtained for an initial concentration of 0.0055 mM (123.2 ppm$_v$ in standard conditions) and a vapor concentration of 0.75 mM. Pengyi et al. [9] obtained conversions of ca. 80% and 40% using a flow rate of 180 L/h (retention time 28.8 seconds) for 10 and 15 ppm$_v$ of initial concentration of toluene, a relative humidity of 35%, and a UV lamp of 254 nm. Barraud et al. [10] developed a new catalyst modified with SO_4^{2-} and they carried out toluene degradation with a flow rate of 12 L/h, an inlet concentration of 110 ppm$_v$, and a relative humidity of 35%. Under these conditions conversions of over 90% were obtained. Jeong et al. [11] used a laminar flow photoreactor and obtained a conversion of 80% for an initial concentration of 20 ppm$_v$, a relative humidity of 40%, and a residence time of 33 seconds.

An apparent catalyst surface of the fluidized bed photoreactor has been estimated using the properties of the particles. The apparent density is 1.39 g/cm^3. The average particle diameter has been calculated by using (1) (x_i weight fraction of particles and d_i diameter), supposing that one half of the particles has a diameter of 0.25 mm and the other half has a diameter of 0.50 mm. Therefore, the average particle diameter is 0.33 mm. Particle sphericity was estimated at 0.73 assuming sand-form particles:

$$d = \frac{1}{\sum_{i=1}^{n} (x_i/d_i)}. \quad (1)$$

As can be seen in Table 1, apparent catalyst surface, corresponding to all particles, in the fluidized bed photoreactor is higher than apparent surface in other kinds of photoreactors. Toluene removal per square meter per second in the fluidized bed photoreactor is similar to the maximum removal achieved by other authors. However, we should bear in mind that flow rates and inlet toluene concentration used in this study are greater than in others which use larger reactor volumes. As a consequence, this technology makes it possible to treat higher flow rates of toluene with suitable conversions in smaller photoreactors.

The photocatalytic degradation rate of the organic contaminants over irradiated TiO_2 fitted L−H kinetics [12–16]. There is only one contaminant in this experiment, and a single-site L−H model is introduced to evaluate photocatalytic degradation rates:

$$R_0 = \frac{k \cdot K \cdot [\mathrm{Tol}]}{1 + K \cdot [\mathrm{Tol}]}, \quad (2)$$

where R_0 is the reaction rate (ppm$_v$ s^{-1}), k the reaction rate constant (ppm$_v$ s^{-1}), and K the Langmuir adsorption constant (ppm$_v^{-1}$).

As Figure 6 shows, the photodegradation of toluene follows a pseudo-first-order kinetic over the range of inlet concentrations tested in the photoreactor. This is in agreement with previous studies [17, 18] indicating that photocatalytic oxidation rates follow first-order kinetics at low concentrations when the term $K \cdot [\mathrm{Tol}]$ is much less than 1.

3.3. Regeneration of the deactivated catalyst

One of the disadvantages of the application of TiO_2 to the photocatalytic decomposition of pollutants in the air is the

Table 1: Comparison of data in the photocatalytic removal of toluene.

Author	Catalyst surface (cm^2)	Reactor volume (L)	Flow rate (L/h)	Inlet toluene concentration (ppm_v)	Relative humidity (%)	Toluene conversion (%)	Toluene removal ($mg/m^2 \cdot s$)
Marcì [8]	864.0	16.3	120	123.2	59*	5	$9.78 \cdot 10^{-3}$
Pengyi [9]	884.4	1.44	180	10	35	80	$1.86 \cdot 10^{-2}$
Pengyi [9]	884.4	1.44	180	15	35	40	$1.40 \cdot 10^{-2}$
Barraud [10]	288.6	0.07	12	110	35	>90	$4.70 \cdot 10^{-5}$
Jeong [11]	356.4	0.55	60	20	40	80	$3.08 \cdot 10^{-5}$
This study	$4.04 \cdot 10^4$**	0.38	300	80	-***	85	$5.76 \cdot 10^{-3}$
This study	$4.04 \cdot 10^4$**	0.38	300	199	-***	77	$1.31 \cdot 10^{-2}$

*Supposed 1 bar of pressure.
**Theoretical (geometric) surface of the particles bed.
***Not measured.

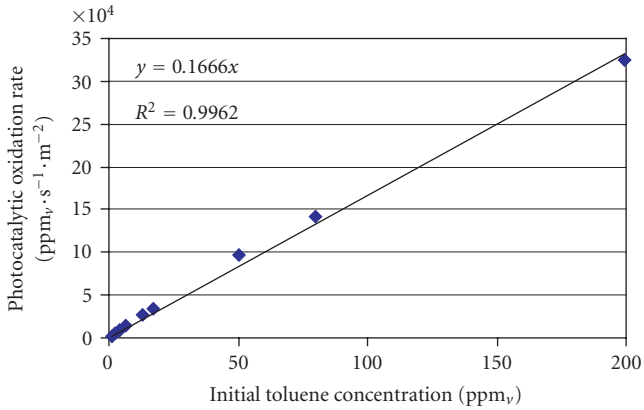

Figure 6: Variation of toluene photocatalytic oxidation rate per square meter of catalyst versus initial toluene concentration.

Figure 7: Activated and deactivated catalysts.

catalytic deactivation that sometimes takes place, due to the strong adsorption of intermediates by active sites on the TiO_2 surface. The catalytic deactivation and coloration that occur during the course of photodecomposition of toluene has been widely reported in the literature [19–22]. The strong interaction between the active sites on the catalyst surface and the oxygen-bearing reaction intermediates leads to an abrupt decrease in the number of active sites during the course of reaction.

It is reported for toluene photo-oxidation that photocatalyst deactivation occurs in the absence of water vapor [23], while for other substrates no deactivation of the photocatalyst was observed under dry conditions even after long periods of irradiation [24]. The color of the catalyst changed from white to light brown (Figure 7) after the photo-oxidation of toluene, indicating that the catalyst had been deactivated. The changed colour of exhausted catalysts is directly associated with the accumulation of those intermediates on the surface, according to the results published in [19–22]. In photocatalytic regeneration, recalcitrant surface species are gradually removed from the photocatalyst through continuous exposure to UV illumination in clean (uncontaminated) flowing air. In general, humidified air is preferred for photocatalytic regeneration because a complete oxidation reaction may be significantly hindered in the complete absence of water. Although, a deactivation study has not been carried out, the regeneration process has been evaluated. Thus, the samples were regenerated in air flow under UV irradiation for 1, 2, 4, and 6 hours, using a fluidized bed photoreactor.

In order to obtain insights on the surface phenomena involved in the reaction, the regeneration processes of deactivated TiO_2 catalyst have been investigated using FT-IR spectroscopy to identify the intermediates adsorbed on the surface of the aggregates of TiO_2 particles. No gas-phase byproducts were detected by online GC/MS under experimental conditions in agreement with other studies [25]. Products remaining on the deactivated aggregates of TiO_2 particles (having a brownish color) were extracted by acetonitrile, dichloromethane (methylene chloride), and isooctane, and were analyzed using GC/MS to identify the intermediates. The deactivated catalyst used in the regeneration processes was obtained by working the photoreactor at high concentrations of toluene and without addition of water vapor in less than 5 hours.

Samples of fresh, deactivated, and regenerated aggregates of TiO_2 particles have been analyzed using FT-IR in order to determine the distribution and features of the hydroxyl groups. The differences between the samples were not significant from 4000 to 2000 cm^{-1} and all the bands appeared in

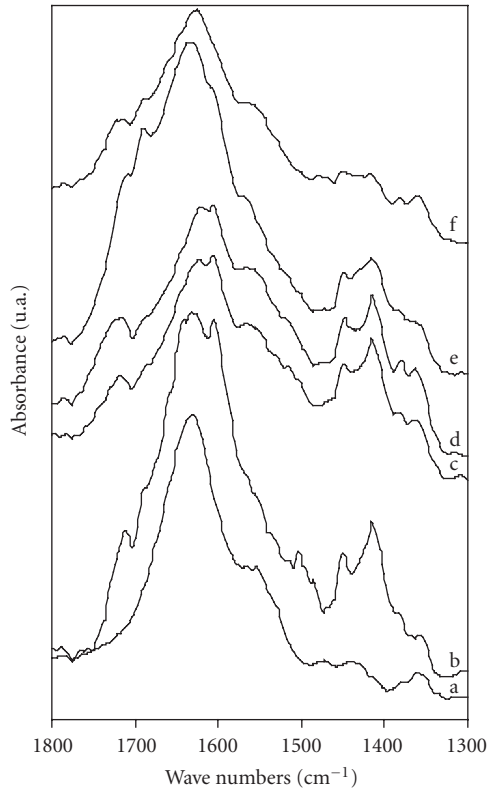

Figure 8: FT-IR spectra of fresh aggregates of TiO_2 particles (a), deactivated aggregates of TiO_2 particles (b), TiO_2 particles regenerated in air flow under UV irradiation for 1 hour (c), 2 hours (d), 4 hours (e), and 6 hours (f) in the region between 1800–1300 cm^{-1}. The spectra have been displaced vertically for clarity.

the same position of fresh aggregates of TiO_2 particles. However, new bands due to adsorbed intermediates appeared in the region from 1600 to 1300 cm^{-1} (Figure 8).

To identify these intermediates, Figure 9 shows the FT-IR spectra of fresh, deactivated aggregates of TiO_2 particles and the sample regenerated in air flow under UV irradiation for 6 hours. Thus, in deactivated samples new bands appear at 1503, 1450, and 1415 cm^{-1} due to vibrations of benzoic acid, according to results published by other authors and detailed assignment of major IR bands [26–28]. The other bands centered on 1675, 1641, and 1604 cm^{-1} are assigned to vibrations of benzaldehyde. These new bands disappear in the FT-IR spectrum when a sample is regenerated in air flow under UV irradiation for 6 hours. By comparing the spectra of fresh and regenerated samples, it can be seen that the regenerated sample in air flow under UV irradiation for 6 hours gives IR bands almost identical to those of the fresh sample. Therefore, benzoic acid and benzaldehyde are believed to be present in deactivated samples.

GC/MS analysis is a clear indication that benzaldehyde is the most important by-product with only trace elements of benzyl alcohol. Nevertheless, in the analysis of the dichloromethane, only extracts of benzaldehyde were detected. Finally, no by-products were detected when isooctane was used as a solvent.

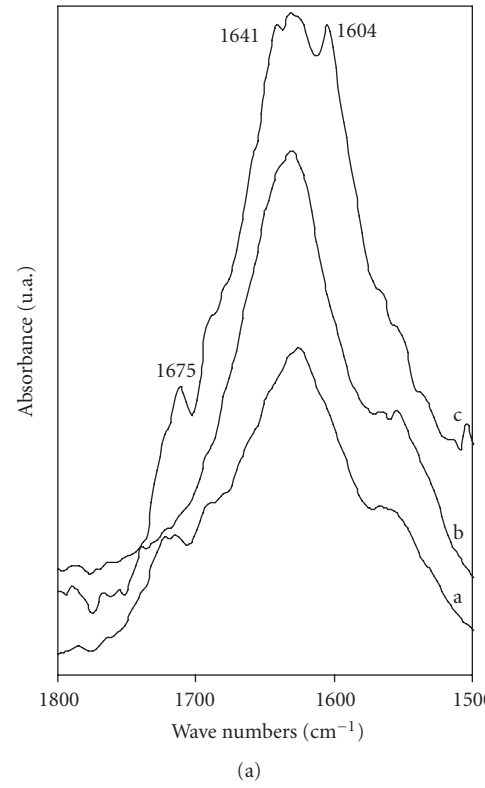

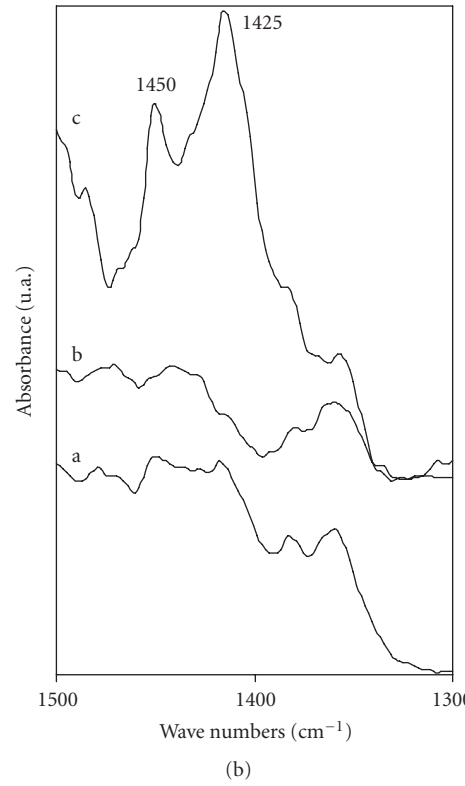

Figure 9: FT-IR spectra of TiO_2 particles regenerated in air flow under UV irradiation for 6 hours (a), fresh aggregates of TiO_2 particles (b), and deactivated aggregates of TiO_2 particles (c) in the region between 1800–1300 cm^{-1}. The spectra have been displaced vertically for clarity.

In summary, benzaldehyde and traces of benzyl alcohol were the by-products detected by GC/MS.

4. CONCLUSIONS

The most significant conclusions of this work can be summarized as follows.

(i) The photocatalytic degradation of toluene in air using aggregates of TiO_2 particles has been carried out successfully in a fluidized bed photoreactor.
(ii) The aggregates of the TiO_2 particles prepared are of a reasonable particle size to be fluidized and are photocatalytically active.
(iii) Relative toluene conversion decreases while increasing the initial toluene concentration in air but it reaches values higher than 77% between 0 and 200 ppm_v of toluene in air.
(iv) Finally, three major toluene intermediates (benzoic acid, benzaldehyde, and benzyl alcohol) were identified.

ACKNOWLEDGMENT

Financial support by the Spanish Ministry of Science and Technology (FIT-310200-2004-226) is acknowledged.

REFERENCES

[1] W. H. Strehlow and E. L. Cook, "Compilation of energy band gaps in elemental and binary compound semiconductors and insulators," *Journal of Physical and Chemical Reference Data*, vol. 2, no. 1, pp. 163–200, 1973.

[2] P. L. Yue, F. Khan, and L. Rizzuti, "Photocatalytic ammonia synthesis in fluidised fluidixed bed reactor," *Chemical Engineering Science*, vol. 38, no. 11, pp. 1893–1900, 1983.

[3] L. A. Dibble and G. B. Raupp, "Fluidized-bed photocatalytic oxidation of trichloroethylene in contaminated airstreams," *Environmental Science and Technology*, vol. 26, no. 3, pp. 492–495, 1992.

[4] T. H. Lim, S. M. Jeong, S. D. Kim, and J. Gyenis, "Photocatalytic decomposition of NO by TiO_2 particles," *Journal of Photochemistry and Photobiology A: Chemistry*, vol. 134, no. 3, pp. 209–217, 2000.

[5] J. Fermoso, O. Prieto, and R. Irusta, "Photocatalytic degradation of gas flow of trichloroethylene (TCE) over TiO_2/sepiolite in a fluidized bed photoreactor," in *Proceedings of the 7th Italian Conference on Chemical and Process Engineering*, vol. 1, pp. 575–580, Giardini di Naxos, Italy, May 2005.

[6] T. H. Lim and S. D. Kim, "Trichloroethylene degradation by photocatalysis in annular flow and annulus fluidized bed photoreactors," *Chemosphere*, vol. 54, no. 3, pp. 305–312, 2004.

[7] G. Martra, "Lewis acid and base sites at the surface of microcrystalline TiO_2 anatase: relationships between surface morphology and chemical behaviour," *Applied Catalysis A: General*, vol. 200, no. 1, pp. 275–285, 2000.

[8] G. Marcì, M. Addamo, V. Augugliaro, et al., "Photocatalytic oxidation of toluene on irradiated TiO_2: comparison of degradation performance in humidified air, in water and in water containing a zwitterionic surfactant," *Journal of Photochemistry and Photobiology A: Chemistry*, vol. 160, no. 1-2, pp. 105–114, 2003.

[9] Z. Pengyi, L. Fuyan, Y. Gang, C. Qing, and Z. Wanpeng, "A comparative study on decomposition of gaseous toluene by O_3/UV, TiO_2/UV and O_3/TiO_2/UV," *Journal of Photochemistry and Photobiology A: Chemistry*, vol. 156, no. 1–3, pp. 189–194, 2003.

[10] E. Barraud, F. Bosc, D. Edwards, N. Keller, and V. Keller, "Gas phase photocatalytic removal of toluene effluents on sulfated titania," *Journal of Catalysis*, vol. 235, no. 2, pp. 318–326, 2005.

[11] J. Jeong, K. Sekiguchi, and K. Sakamoto, "Photochemical and photocatalytic degradation of gaseous toluene using short-wavelength UV irradiation with TiO_2 catalyst: comparison of three UV sources," *Chemosphere*, vol. 57, no. 7, pp. 663–671, 2004.

[12] A. Bouzaza and A. Laplanche, "Photocatalytic degradation of toluene in the gas phase: comparative study of some TiO_2 supports," *Journal of Photochemistry and Photobiology A: Chemistry*, vol. 150, no. 1–3, pp. 207–212, 2002.

[13] J. M. Coronado, M. E. Zorn, I. Tejedor-Tejedor, and M. A. Anderson, "Photocatalytic oxidation of ketones in the gas phase over TiO_2 thin films: a kinetic study on the influence of water vapor," *Applied Catalysis B: Environmental*, vol. 43, no. 4, pp. 329–344, 2003.

[14] E. Obuchi, T. Sakamoto, K. Nakano, and F. Shiraishi, "Photocatalytic decomposition of acetaldehyde over TiO_2/SiO_2 catalyst," *Chemical Engineering Science*, vol. 54, no. 10, pp. 1525–1530, 1999.

[15] N. O. Timothy, "Photooxidation of sub-parts-per-million toluene and formaldehyde levels on titania using a glass-plate reactor," *Environmental Science & Technology*, vol. 30, no. 12, pp. 3578–3584, 1996.

[16] H. Liu, Z. Lian, X. Ye, and W. Shangguan, "Kinetic analysis of photocatalytic oxidation of gas-phase formaldehyde over titanium dioxide," *Chemosphere*, vol. 60, no. 5, pp. 630–635, 2005.

[17] M. Keshmiri, M. Mohseni, and T. Troczynski, "Development of novel TiO_2 sol-gel-derived composite and its photocatalytic activities for trichloroethylene oxidation," *Applied Catalysis B: Environmental*, vol. 53, no. 4, pp. 209–219, 2004.

[18] S. Upadhya and D. F. Ollis, "A simple kinetic model for the simultaneous concentration and intensity dependencies of TCE photocatalyzed destruction," *Journal of Advanced Oxidation Technologies*, vol. 3, no. 2, p. 199, 1998.

[19] M. L. Sauer, M. A. Hale, and D. F. Ollis, "Heterogenous photocatalytic oxidation of dilute toluene-chlorocarbon mixtures in air," *Journal of Photochemistry and Photobiology A: Chemistry*, vol. 88, no. 2-3, pp. 169–178, 1995.

[20] Y. Luo and D. F. Ollis, "Heterogeneous photocatalytic oxidation of trichloroethylene and toluene mixtures in air: kinetic promotion and inhibition, time-dependent catalyst activity," *Journal of Catalysis*, vol. 163, no. 1, pp. 1–11, 1996.

[21] S. A. Larson and J. L. Falconer, "Initial reaction steps in photocatalytic oxidation of aromatics," *Catalysis Letters*, vol. 44, no. 1-2, pp. 57–65, 1997.

[22] H. Einaga, S. Futamura, and T. Ibusuki, "Heterogeneous photocatalytic oxidation of benzene, toluene, cyclohexene and cyclohexane in humidified air: comparison of decomposition behavior on photoirradiated TiO_2 catalyst," *Applied Catalysis B: Environmental*, vol. 38, no. 3, pp. 215–225, 2002.

[23] S. Sitkiewitz and A. Heller, "Photocatalytic oxidation of benzene and stearic acid on sol-gel derived TiO_2 thin films attached to glass," *New Journal of Chemistry*, vol. 20, no. 2, pp. 233–241, 1996.

[24] W. A. Jacoby, D. M. Blake, R. D. Noble, and C. A. Koval, "Kinetics of the oxidation of trichloroethylene in air via heterogeneous photocatalysis," *Journal of Catalysis*, vol. 157, no. 1, pp. 87–96, 1995.

[25] O. d'Hennezel, P. Pichat, and D. F. Ollis, "Benzene and toluene gas-phase photocatalytic degradation over H_2O and HCL pretreated TiO_2: by-products and mechanisms," *Journal of Photochemistry and Photobiology A: Chemistry*, vol. 118, no. 3, pp. 197–204, 1998.

[26] R. Méndez-Román and N. Cardona-Martínez, "Relationship between the formation of surface species and catalyst deactivation during the gas-phase photocatalytic oxidation of toluene," *Catalysis Today*, vol. 40, no. 4, pp. 353–365, 1998.

[27] V. Augugliaro, S. Coluccia, V. Loddo, et al., "Photocatalytic oxidation of gaseous toluene on anatase TiO_2 catalyst: mechanistic aspects and FT-IR investigation," *Applied Catalysis B: Environmental*, vol. 20, no. 1, pp. 15–27, 1999.

[28] L. Cao, Z. Gao, S. L. Suib, T. N. Obee, S. O. Hay, and J. D. Freihaut, "Photocatalytic oxidation of toluene on nanoscale TiO_2 catalysts: studies of deactivation and regeneration," *Journal of Catalysis*, vol. 196, no. 2, pp. 253–261, 2000.